INL/CON-16-37834
PREPRINT

ACCELEROMETERS IN FLOW FIELDS: A STRUCTURAL ANALYSIS OF THE CHOPPED DUMMY IN-PILE TUBE

ANS 2016

T. K. Howard, W. R. Marcum, G. D. Latimer,
A. Weiss, W. F. Jones, A. M. Phillips,
N. Woolstenhulme, K. Holdaway, J. Campbell

June 2016

The INL is a
U.S. Department of Energy
National Laboratory
operated by
Battelle Energy Alliance

ACCELEROMETERS IN FLOW FIELDS: A STRUCTURAL ANALYSIS OF THE CHOPPED DUMMY IN-PILE TUBE

T. K. Howard[†], W. R. Marcum[‡], G. D. Latimer, A. Weiss
Department of Nuclear Science and Engineering
Oregon State University
3451 SW Jefferson Way, Corvallis, OR
[†]howartre@oregonstate.edu; [‡]wade.marcum@oregonstate.edu

W. F. Jones[*], A. M. Phillips, N. Woolstenhulme, K. Holdaway, J. Campbell,
Idaho National Lab
2525 Fremont Ave, Idaho Falls, ID
[*]warren.jones@inl.gov

ABSTRACT

Four tests characterizing the structural response of the Chopped-Dummy In-Pile tube (CDIPT) experiment design were measured in the Hydro-Mechanical Fuel Test Facility (HMFTF). Four different test configurations were tried. These configurations tested the pressure drop and flow impact of various plate configurations and flow control orifices to be used later at different reactor power levels. Accelerometers were placed on the test vehicle and flow simulation housing. A total of five accelerometers were used with one on the top and bottom of the flow simulator and vehicle, and one on the outside of the flow simulator. Data were collected at a series of flow rates for 5 seconds each at an acquisition rate of 2 kHz for a Nyquist frequency of 1 kHz. The data were then analyzed using a Fast Fourier Transform (FFT) algorithm. The results show very coherent vibrations of the CDIPT experiment on the order of 50 Hz in frequency and 0.01 m/s^2 in magnitude. The coherent vibrations, although small in magnitude pose a potential design problem if the frequencies coincide with the natural frequency of the fueled plates or test vehicle. The accelerometer data was integrated and combined to create a 3D trace of the experiment during the test. The merits of this data as well as further anomalies and artifacts are also discussed as well as their relation to the instrumentation and experiment design.

KEYWORDS
accelerometers; FIV, FSI, vibration

1. INTRODUCTION

With the advent of the Global Threat Reduction Initiative (GTRI) presented by the National Nuclear Security Agency (NNSA), there has been a push to convert the highly enriched uranium (HEU) in test and research reactor to low enriched uranium (LEU). For some reactors the process is as easy as adding more LEU elements in lieu of the HEU ones. However, some High Performance Research Reactors (HPRR's) cannot simply add more fuel elements to maintain criticality, let alone and economically viable neutron density. In order for some HPRR's to achieve a reasonable neutron density, new fuel elements need to be designed and tested. The Hydro Mechanical Test Facility (HMFTF) at Oregon State University (OSU) is a thermal hydraulic test loop that is designed to allow a variety of single, full-scale HPRR fuel elements to be tested. It provides part of the experiment design process, to test and aid in the design of experiments out-of-pile prior to in-pile testing in the Advanced Test Reactor (ATR) at the Idaho National Lab (INL).

The HMFTF allows for more insight as to the flow phenomena experienced by test elements. An advantage of testing in the HMFTF, as opposed to in-pile testing, is the HMFTF provides data beyond the simple pressure drop seen information which can in turn be used for the development of heat transfer correlations and safety analysis. The experiment and results detailed herein are specifically done for the Chopped Dummy In-Pile Tube (CDIPT) experiment. The results provided aid in the design and development of the new fuels as well as post irradiation analysis of the elements.

Since the geometry is similar to concentric cylinders, one could make this assumption and calculate the expected frequencies from the cylinder vibrations [2], however the flow for CDIPT is more complex as plate fluctuations and internal flow can affect the overall vibration. Previous analysis of in-pile experiments have shown limited analysis of complex flow geometries can result in failure [1].

2. EXPERIMENTAL SET UP

All testing was performed in the HMFTF. The HMFTF is a flow loop designed to emulate the flow characteristics of a wide range of nuclear reactors. The HMFTF consists of a closed primary loop containing a separate bypass leg and secondary loop. The purpose of the primary loop is to control the system fluid (water) at a prescribed temperature, flow rate, and pressure in order to examine the response of the test specimen located in the test section of the primary loop. The secondary loop is a feed water system is to prepare the primary fluid (pH and conductivity), and account for all necessary heat removal and fluid makeup requirements that may be required for the primary loop. The test section in the primary loop accommodates the insertion of test elements, the CDIPT being one such element. For CDIPT testing, experiments were run at flow conditions based on the ATR at INL. Table I lists the values of the state properties for all tests.

Table I. List of test conditions

Property	Value
pH	5 – 7
Fluid Conductivity [μS/cm]	< 100
System Pressure [psi (MPa)]	360 ± 5 (2.482 ± 0.034)
Fluid Temperature [°F (°C)]	150 ± 5 (65.6 ± 2.8)

For testing, capsules were placed inside a vehicle. The vehicle is then placed inside a flow simulator which creates conditions similar to those seen in-pile. The flow simulator is then placed inside the test section pipe and placed into the HMFTF. The vehicle itself contains two different slots containing five capsules each. For every test, each slot contained an orifice spacer, and two capsules with plates (one with Hafnium Rings) and two capsule spacers (capsules without plates). The capsule spacer is the generic capsule without plates. The capsules containing plates contain eight equally sized aluminum plates with four plates placed on top of the other four in the z-direction (direction of flow). Some capsules contained four hafnium rings as a modification to the design. The final component was the orifice spacer which was a capsule consisting of a single circular hole designed to achieve specific flow rates at give pressure drops across the test section. The components can be seen in Figure 1.

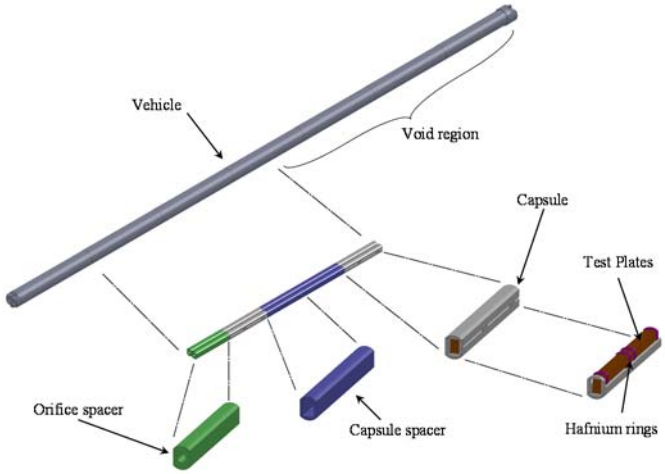

Figure 1. Vehicle Components

A total of four tests were conducted with five accelerometers for structural response characterization. The four tests consisted of three different arrangements of the vehicle components, herein referred to as geometric configurations (GC's). A graphic of GC's is shown in Figure 2.The first two tests, 002 and 003, used the GC1 layout. Test 004 and 005 used GC2 and GC3 respectively. Emulation of testing in-pile is represented by GC1 for medium power, GC2, for high power, and GC3 as a proposed alternative configuration of flow testing at medium power.

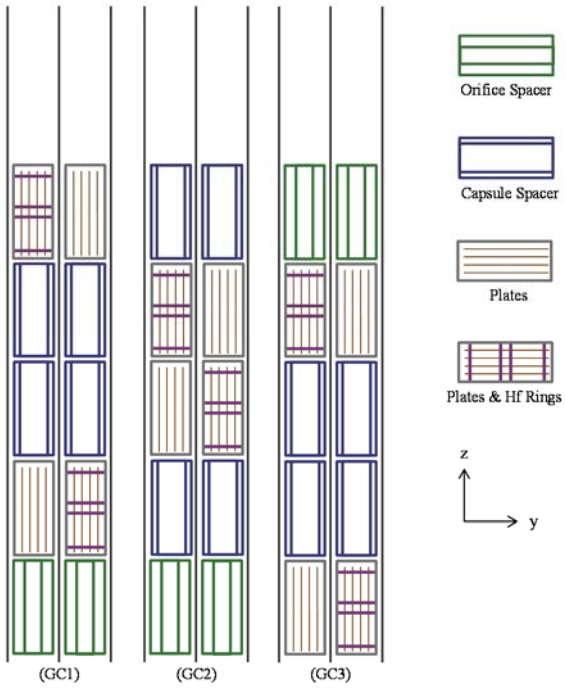

Figure 2. CDIPT Arrangement.

Testing began by increasing the flow until a pressure drop of 40 psi (276 kPa) across the vehicle was maintained. Data was sampled at a frequency of 2 Hz. Once data had been sampled for at least two minutes, a burst was conducted. The burst lasted for five seconds and collected data at a frequency of 2 kHz.The sampling rate and duration were chosen because they were antipated to sufficiently capture the vibrational frequnecies of the system and safely avoided the limitations of data recording space. After the burst was complete, the flow rate was increased by no more than 5 gpm ($3.2x10^{-4}$ m^3/s). The process of holding the flow rate, bursting, and raising the flow rate incrementally was repeated until a final differential pressure of 130 psi (896 kPa) was achieved. Once the final step was achieved, the pump and valve setting were returned to that of the first step. In doing so the flow rate should be the same as the first step. This step was performed to ensure continuity of the system and observe that no hysteresis had occurred over the duration of the test.

To analyze the structural response of the system, five accelerometers were used. The accelerometer signals were labeled as VT-40Xx. X is the number of the accelerometer and x is the direction. The accelerometers used have an inherent direction e.g. x with respect to the accelerometer is always away from the wire. Because the accelerometer orientation was different than the global coordinate system, the direction of the accelerometers are labeled as a, b, and c to avoid confusion as to whether the frame of reference was a global or local system. Global x corresponds to a, y to b, and z to c. Two accelerometers were placed on the vehicle (at the top and bottom) and three were placed on the flow simulator (top, bottom and middle). The accelerometer positions can be seen in Figure 3.

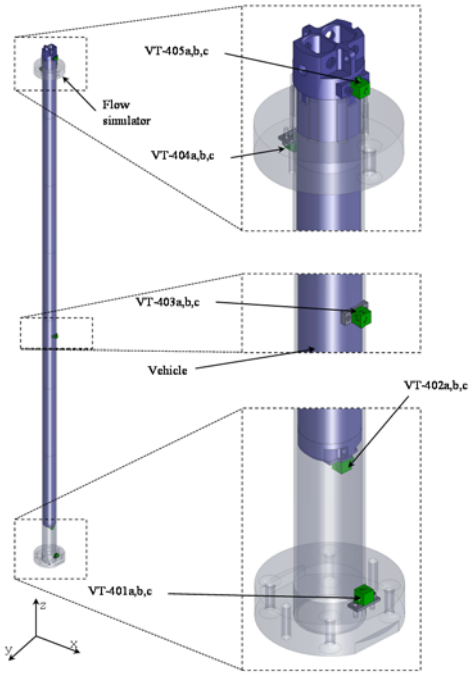

Figure 3. Accelerometer Locations.

Data for the accelerometers was collected over the entirety of the test, however the pertinent data of the test was collected during the burst. The burst being at 2 kHz allowed for a Nyquist frequency of 1 kHz.

3. DATA PROCESSING

Two areas of interest were looked at from the accelerometer data. First the raw accelerometer data was analyzed with an FFT so that acceleration frequencies and magnitudes could be analyzed directly, and second was a reconstruction of the position profile of the accelerometers over the course of the burst.

A spectral analysis was conducted on each accelerometer channel at each respective flow rate over the burst set using the Fast Fourier Transform method (FFT). The FFT data was calculated using a buffered bin size eight times larger than the size of the data set to the next power of two. This was done to increase the accuracy of the magnitudes of the FFT as well as better locate the specific frequencies. In order to avoid spurious magnitudes and frequencies created by drift, a fourth-order polynomial was fit to, and subtracted from the burst data set. Using a fitted polynomial prevents very low order frequencies (drift and offset) from creating noise in the higher frequency domain, as would be the case if low frequency data were removed or ignored.

While the acceleration data is important and the means of measuring vibrations, position data is more useful from a structural analysis perspective. The position is obtained from the integration of the acceleration data.

$$x = \iint a \cdot dt^2 \tag{1}$$

Since information of the acceleration is obtained through sampling, the function driving the acceleration is unknown integration must be performed numerically. Before the numerical method is discussed, it is important to acknowledge the implications of numerical integration. Consider for a moment, an object accelerating harmonically at a given frequency, f . The oscillation can be described with a given amplitude, A, and phase, φ. The equation describing such a system,

$$a = A\cos(2\pi ft + \varphi), \tag{2}$$

can then be integrated to determine the position. By placing equation (2) in equation (1) and performing the integration over a time t , a solution is obtained for the position. The solution,

$$x = -\frac{A}{4\pi^2 f^2}\cos(2\pi ft + \varphi) + C_1 \mathrm{t} + C_2, \tag{3}$$

from this approach has a key problem. There is both an offset and linear drift if the coefficients of integration are not chosen correctly. If the system is constrained (as it should be), the coefficients will be zero. Since the integration is performed numerically and assumes the antiderivative is 0 at time 0, the coefficients will not necessarily be zero, but rather the position,

$$x = -\frac{A}{4\pi^2 f^2}\cos(2\pi ft + \varphi) - \frac{A}{2\pi f}\sin(\varphi)\,\mathrm{t} + \frac{A}{4\pi^2 f^2}\cos(\varphi), \tag{4}$$

contains at least one non-zero coefficient regardless of the phase. Because of the aforementioned conditions, boundary conditions need to be appropriately applied. Since the explicit function is not known at the initial time, some other boundary condition must be determined. What is known is that both the average velocity and the average position over an infinite time should nil, or can be approximated as nil, if the sample length (T) is sufficiently long, thus

$$\frac{\int_0^T v \cdot dt}{T} \simeq \frac{\int_0^T x \cdot dt}{T} = 0 \ , \tag{5}$$

can be used as boundary conditions to remove the offset and the linear drift. Applying the condition in equation (5) to equation (4) produces a corrected equation for the position of,

$$\mathrm{x} = -\frac{A}{4\pi^2 f^2}\cos(2\pi ft + \varphi) + \frac{A}{4T\pi^2 f^2}\cos(2\pi fT + \varphi)\left(t - \frac{T}{2}\right) + \frac{A}{8T\pi^3 f^3}\sin(2\pi fT + \varphi), \tag{6}$$

which is now a function of the sample length. Unfortunately equation (6) is not without error. While reduced in magnitude, the linear and offset errors are still present. To compensate, a linear polynomial can be fit to the data, thus resulting in a reduction in the error terms.

It is important to point out that any order of adjustment done to the acceleration will produce two orders higher of error in the position due to the error. Hence, the 4th order polynomial fit performed in the acceleration FFT analysis, would require a minimum of a 6th order correction on the position data, or 5th order correction on the velocity. For the integration form acceleration to position, the acceleration data was corrected for drift with a 2nd order polynomial, the velocity with a 3rd order polynomial and the position with a 4th order polynomial.

The actual integration was performed using a trapezoid method of integration. Trapezoid method was chosen because the scheme doesn't result in the loss of data points. Maintaining the same number of data points is important to see higher frequency data. If Simpsons rule (or another second order scheme) were used the number of points would be cut in half after each integration. The Nyquist frequency for the position data set would then be reduced to 250 Hz. The downside to this method of integration is error can be relatively high since a linear fit is being used for "curvy" data. To reduce the error experienced by the trapezoid scheme, a spline fit was used to increase the resolution of the data. The spline fit increased the data resolution by a factor of 100. The order of magnitude increase was chosen so the highest frequency components would experience a small loss (<1%) in in relative magnitude of a clean signal.

While the above procedure is appropriate for ideal oscillation data, it doesn't work if there is noise in the system even if the signal to noise ratio is as high as 1000. The reason for the failure is the double integration of white noise. The integration of white noise causes a red shift in the FFT spectrum producing Brownian noise. The noise, be it signal noise or higher frequency accelerations caused by turbulence, is seen as a random mix of low and high order frequencies in the FFT data. Noise around the peaks of interest and higher frequency noise isn't a problem, but lower frequency noise causes issues upon integration of the data. The reason being is integration of the data, in some ways acts as a low pass filter. Looking back at equation (3), the integration of any oscillation results in a magnitude which is proportional to the inverse of the frequency squared.

To account for the noise, a high-pass, low-pass, and noise specific filter were used. The filters were performed by converting the time domain to the frequency domain via the use of an FFT. The high-pass and low-pass filters were identical in their implementation. The filter equation,

$$A_{fft}'(f)=\begin{cases}0, & if \quad f \le f_{low}\\ A_{fft}(f), & if \ f_{low} < f < f_{high}\\ 0, & if \quad f \ge f_{high}\end{cases}, \tag{7}$$

sets the new amplitude of the FFT, A'_{fft}, to 0 if it falls below the lower cutoff frequency, f_{low} (10 Hz) or the higher frequency, f_{high} (1000 Hz). Anything in between maintained the magnitude of the original FFT amplitude, A_{fft}. The choice of 1000 Hz was because anything above the Nyquist frequency wasn't realistic. The only reason frequencies above 1000 Hz existed were because the original data was spline fit to increase the resolution. The lower cutoff frequency was chosen somewhat arbitrarily based on the frequencies seen from the accelerometer data, i.e. it need to be chosen so that dominant peaks were not being cut. 10 Hz was ultimately chosen because it reduced the offset error seen in equation (6) to less than 2.5% of a corresponding oscillation on average.

The filter is reasonably effect, but still produces issues at the lower end of the frequency spectrum. To account for this, a noise specific filter was implemented. The filter looked at the non-zeroed data from equation (7) and took the average and standard deviation of it. If the data was greater than three standard deviations from the mean it was not considered to be noise.

$$A_{fft}'(f)=\begin{cases}A_{fft}(f), & if \ A_{fft}(f) > A_{cutoff}\\ A^2{}_{fft}(f)/A_{cutoff}, & if \ A_{fft}(f) \le A_{cutoff}\end{cases}, \tag{8}$$

The final aspect of the noise filter eliminated the 60 Hz and corresponding 180 Hz peaks by cutting off the peak over a 2 Hz window. That is to say the frequency magnitude from 59 Hz to 61 Hz was simply reset to the frequency at 59 Hz.

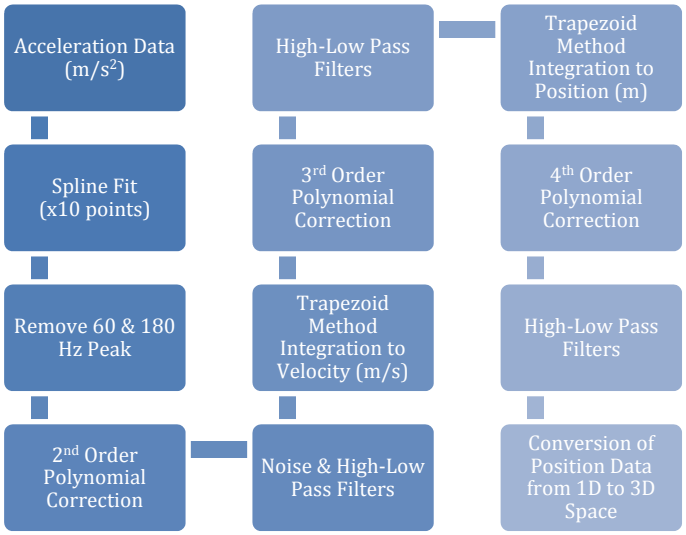

Figure 4. Data Processing Flow Chart.

In the cases where only an FFT was presented, in order to avoid spurious magnitudes and frequencies created by drift, a fourth-order polynomial was fit to, and subtracted from the burst data set. Using a fitted polynomial prevents very low order frequencies (drift and offset) from propagating to higher domains as would be the case if low frequency data were removed or ignored. To obtain further information, the plots

were zoomed into the 200 Hz range. This range on an FFT is important as the change in position is proportional to the inverse frequency squared times the acceleration, or

$$x \propto a \frac{1}{f^2} \tag{9}$$

In some instances, large transients in some flow rates precluded important information from being seen in the zoomed data. Only data where jerk (j),

$$j = \frac{dx}{dt^3} \tag{10}$$

calculated numerically as

$$j \approx \frac{\Delta a}{\Delta t} \tag{11}$$

retained a maximum absolute value less than twenty times the absolute mean value were used for the zoomed plots.

4. RESULTS

While the results for all the four tests were processed [3], only the results from the first structural characterization test is presented.. Figure 5 shows the FFT results from Test 002. Due to the sheer quantity of data only one test was chosen to discuss in detail. The specific test was chosen because it had the most unique test data and VT Signals similar to other tests.. In Figure 5 the x signal is aligned on the left column, the y signal in the center, and the z signal on the right. The rows correspond to the VT number e.g. row 3 is VT-003. Additional titles have been put over each plot for the readers convenience. The cireterion based on equation (11) was used to determine which FFTs to plot.

The same criterion was not used for the final two figures, Figure 6 and Figure 7 which examine the differences between the oscilations observed in the vehicle and the oscillations observed in the flow simulator. The figures were produced using the integration method show in Figure 4, only the midle 5th of the integration is shown. This is done to show the general shapes and avoid presenting additional numerical errors due to the numerical intergration discussed in equation (6).

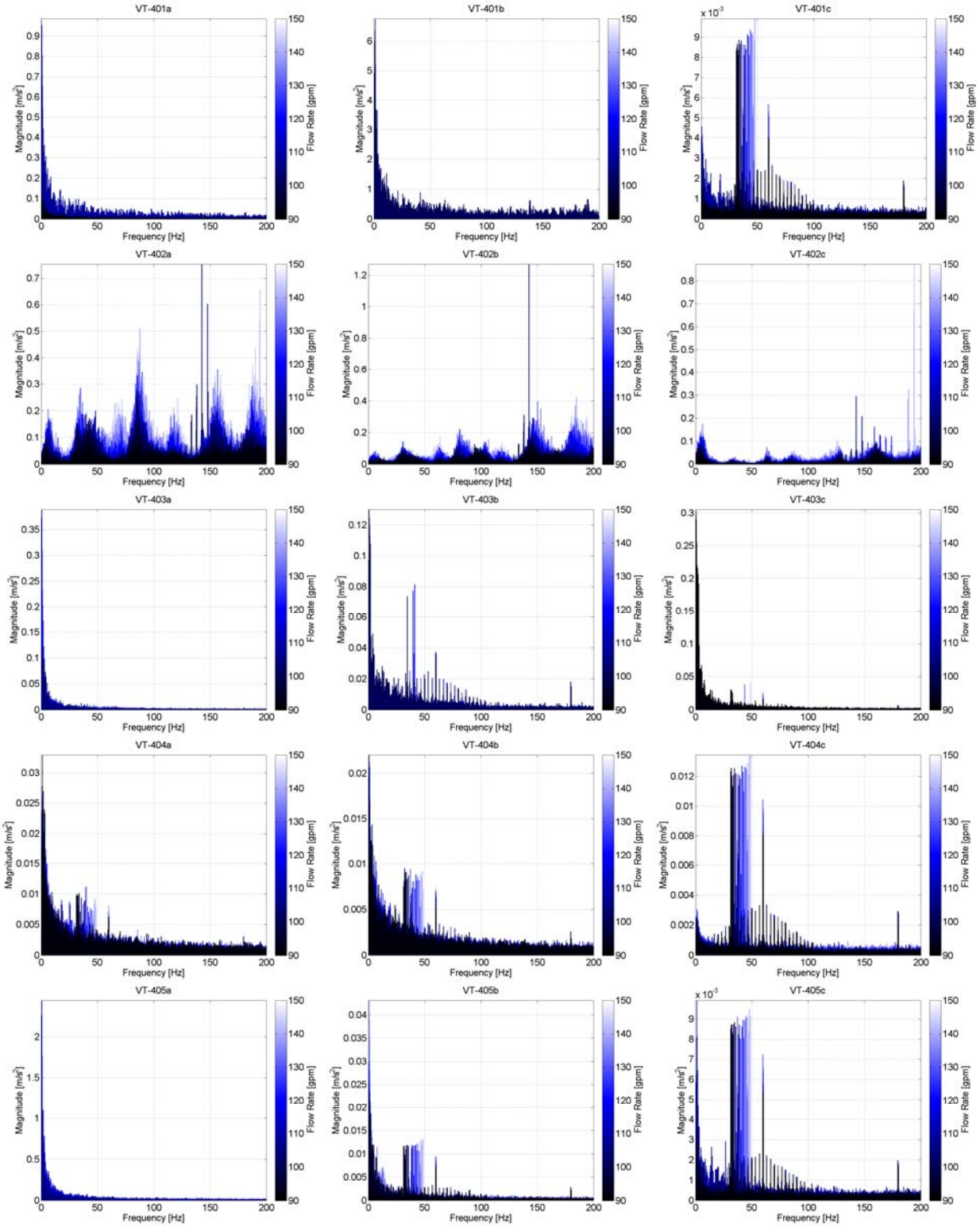

Figure 5. Test 002 Accelerometer FFT.

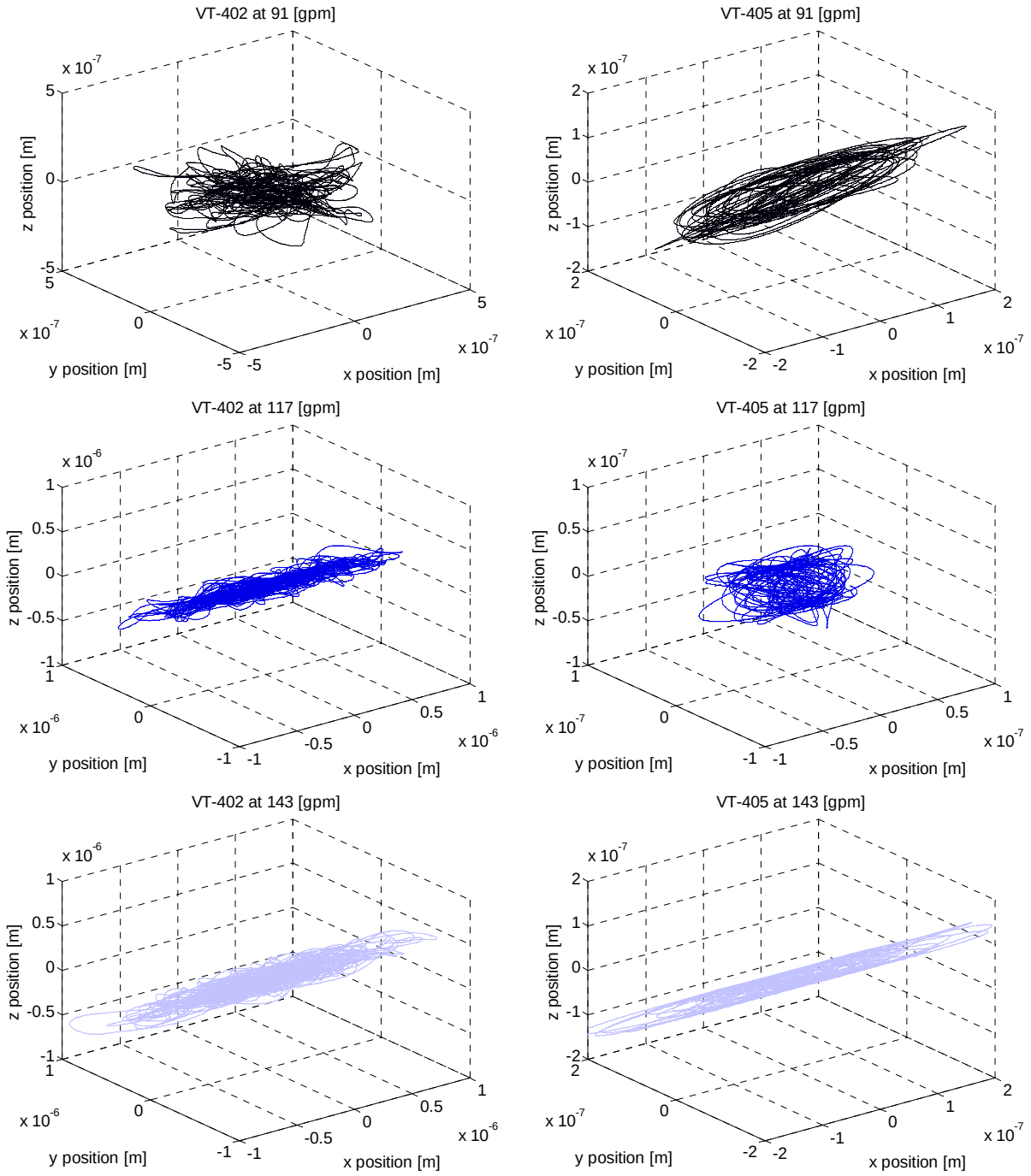

Figure 6. 3D Trace of Test 002 for the Vehicle.VT-402 (left) and VT-405(right) at low(top) medium(middle) and high(top) flow rates

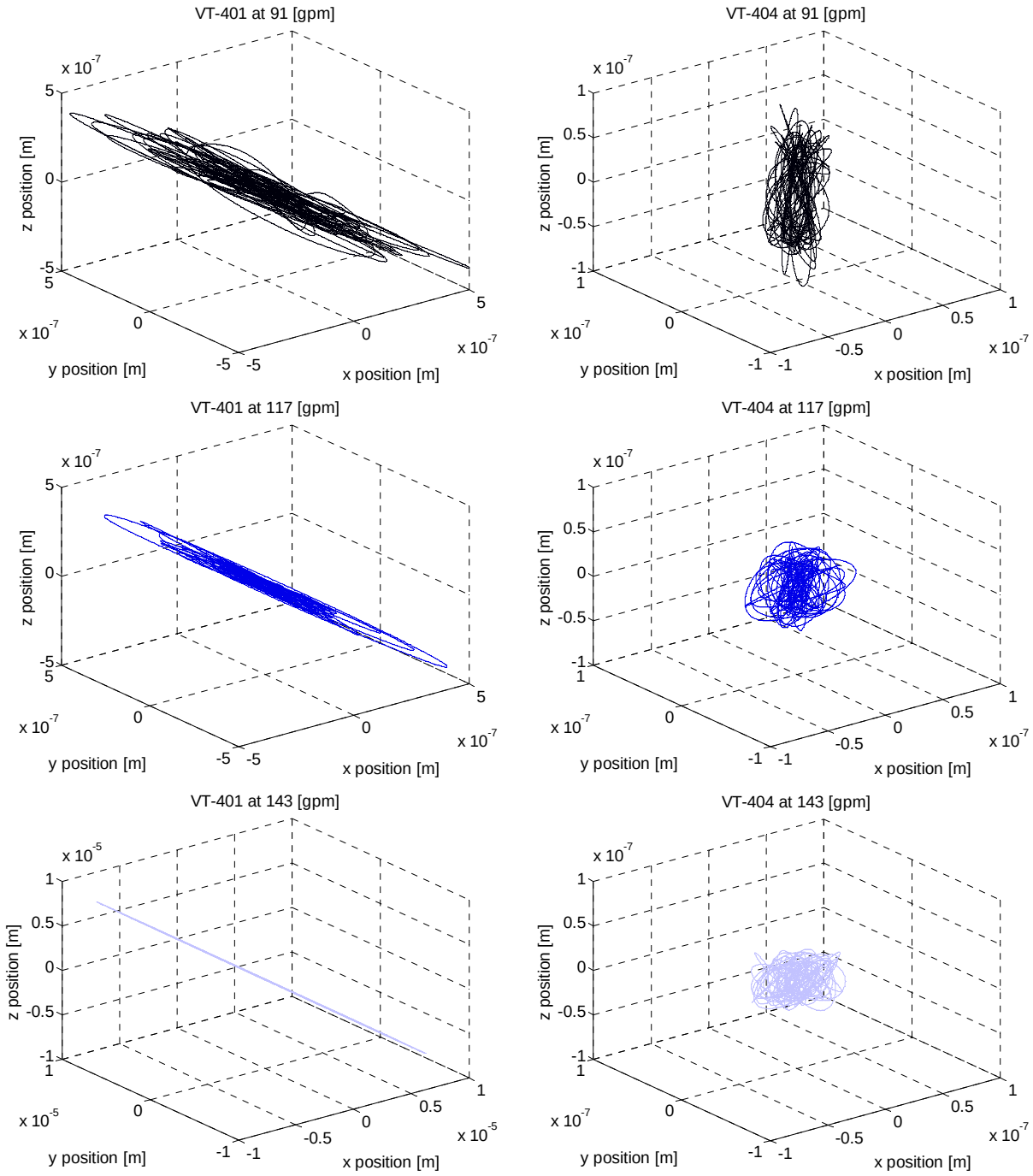

Figure 7. 3D Trace of Test 002 for the Flow Simulator.VT-401 (left) and VT-404(right) at low(top) medium(middle) and high(top) flow rates

5. DISCUSSION

As mentioned earlier, Figure 5 demonstrates the spectrum of plots ranging from 0 to 200 Hz frequencies for applicable signals for signals that lent themselves to FFT analysis. In some cases, quick unstedy frequencies manifested a low order noise washing out any coherent data. These were eliminated from by comparison of the average jerk of the system to the maximum jerk. If the value of the maximum was

more than twenty times the mean, the data was not plotted (the choice was shown to eliminate false low order FFT signals while preserving semi-coherent FFT signals).

A common trend to all plots is a peak at 60 and 180 Hz. The peaks are a consequence of the 60 Hz A/C current of the pump and the corresponding odd harmonics. The peak can be ruled out as being non-physical due to its constant magnitude over all flow rates and constant value A secondary pyramid shape exhibiting sub peaks at 3 Hz or 6 Hz intervals centered on the 60 Hz peak is also seen however, this structure is only seen in some cases at low flow rates. These signals were elimintated for the integration of the acceleration data to provide the postion data.

Another coherent vibration is clearly present for all tests, ergo all geometric configurations, and for a majority of the accleartion signals. These vibrations occur at approximately 50 Hz and a magnitude on the order of 0.01 m/s^2. The structures are best seen in VT-404c from Test 002. The magnitudes very clearly increase with flow rate as does the frequency of the vibrations seen in the FFT plot. What is important to note is the magnitude is nearly identical for all directions. These vibrations are important because they are very coherent as opposed to incoherent oscillations. These vibrations could very well correspond to vibrations in the plate elements due to the smaller magnitude, or may be general vibration of the CDIPT system (it should be noted these vibrations are not seen in other similar HMFTF tests). If it is the former, vibration of plate systems could be potentially characterized by external vibrational analysis. These peaks could easily exist for all accelerometer signals. Given their approximate magnitudes, the signals they are not visible in, they would exists within the noise, or a larger peak.

Another common trend observed in a significant number of the plots is a virtually incoherent signal with a large lower order frequency noise. The accelerometers presenting this trend had similar profiles to others that had previous been eliminated. That is to the say the accelerometer signal, as opposed to providing a clean signal has a series of jumps in them likely caused physically, but providing difficulties in using an FFT analysis to determine any coherent sturcutres. The irregularities in the jumps prevent the FFT method from woking sutibally. A potential work around for this effect is to use a rolling fft to sample pieces of the signal instead of the whole signal. In doing this one could utilize a signal discrimination method like the one applied in Figue 5. The down side is, due to the reduced number of data points, combined with the averaging of the FFT, the clean peaks seen in Figure 5 begin to smear across. This approach was tried but didn't present any additional insight.

A wholly unique FFT signal can be seen in VT-402. VT-402 for reference is the bottom of the vehicle. The unique signal for this VT isn't too much of a surprise. The vehicle rests on top allowing the bottom of the vehicle a large degree of freedom. The increased freedom at the bottom of the vehicle allows for a much more complex signal. Since the vibration of the bottom of the vehicle is influenced by the expantion from the elements into the flow simulator, a variety of higher frequency coherent structures are seen. Althogh not seen in figure 5, these structures continue up to the Nyquist frequency.

The last set of two figures (Figure 6 and Figure 7) look at the integration of the VT signal from acceleration to position. The oscillations occur roughly on the order of a micrometer or less. The signal present produces semi-coherent shapes, but unfortunately is slightly corrupted with lower frequency noise which was seen in the post integration FFT analysis of the data. Figure 6 and Figure 7 examine the oscilations in the vehicle and flow simulator respectively. The left side of each figure is the bottom of the element where the right is at the top. Keeping this in mind, there are some important observations that can be made.

Comparing the top of an element to the bottom, there is a significant difference in the magnitude of the oscillations between the two. The top for both the vehicle and the flow simulator has oscillations an order of magnitude greater than the top. Because of the significant difference between the magnitudes of

oscillations, the top is acting as a pivot point compared to the large fluctuations at the bottom as opposed to a concentric oscillation or modal vibration of the elemtents within the test section.

There are further differences in the shaping of the oscillations as well. The oscilations of the top and bottom of the vehicle are similar in direction, especially at the high flow rate. Both of which being relatively centered at top and fluctuating primarily in the x direction on the bottom. On the otherhand, the flow simulator top and bottom patterns are substantially different. The shape of oscillations of the flow simulator are much more centered at the top and sweep much more at the bottom along an angle as opposed to favoring a particular diection.

One should also note the geometric difference between the flow simulator and the vehicle, the flow simulator rests in the test section on bottom while the vehicle rests in the flow simulator on top. With that being said, the primary swings of the bottom of the elements are at approximately at a 45 degree angle from one another as opposed to being entire in sync, or perpendicular to one another. Returning to Figure 5, this observation can also be seen in the FFT plots. VT-402 has a unique signal, where as VT-401 is very similar to VT-404 and VT-405.

A final observation can be made between the high and low flow rates. In general, as was seen in Figure 5, the magnitude of the oscillations increases with flow except at the top of the flow simulator. In this case the oscillations are small possibly due to a higher frequency in the oscillations. In this case the higher frequencies don't sufficiently increase in magnitude resulting in a tigher oscillation about the center as opposed to an increase in oscillations as seen in the other accelerometers.

6. CONCLUSIONS

The data was collected for four different geometric configurations of the CDIPT experiment and the vibrational frequencies at different locations were analyzed at five different locations on the experiment. Coherent vibrations were seen starting at around 30 Hz and 0.008 m/s^2 for the lowest flow rate which increased 0.016 m/s^2 at 60 Hz for the maximum flow rate seen. Additional artifacts and anomalies have also been addressed.

The results of Test-002, the first structural characterization flow test have been presented in detail. An FFT analysis was performed on the test to look for coherent vibrations within the test. The accelerometer data was then further integrated to determine the priniciple directions and shapes underwhich the oscillations of the CDIPT assembly was occuring. In doing this, a methodology for integrating the accelerometer was chosen and justified to provide reasonable results.

The results will be used for future testing and post-irradiation analysis. Because of the shifting low frequency peak, corresponding flow rates that align with the fundamental frequencies of components should be avoided.

While the algorithm to get from position does what it was intended to do, there are still issues associated with lower order frequencies appearing in the final position data. The question remains as to what degree of physicality this data has. One potential option is raising the cutoff frequency which produces more coherent data, but at the risk of forcing smaller profile shapes which may not capture lower frequencies that may be in fact physical. Another alternative would be averaging the FFT windows over a smaller time frame. The disadvantage of this is the phase can then shift and that data begins to smear. The shaping of would be coherent, however, the end result may be an incorrect shape.

ACKNOWLEDGMENTS

7. REFERENCES

1. N.E. Wolstenhumle, "AFIP-6 MKII First Cycle Report", INL/EXT-12-25170, Idaho National Lab, Idaho Falls (2012)
2. S.S. Chen, *Flow Induced Vibrations of Circular Cylinders*, pp. 112-140, Hemisphere Publishing Corporation, New York, New York, USA (1987).
3. T.K. Howard, "Miniplate 1, Chopped Dummy In-Pile Tube – Test Data Analysis Report", OSU-HMFTF-997002-TECH-003, Oregon State University, Corvallis (2015)